ACCURACY EVALUATION OF TERRESTRIAL LIDAR AND MULTIBEAM SONAR SYSTEMS MOUNTED ON A SURVEY VESSEL

By

MICHAEL ESTEN DIX

A THESIS PRESENTED TO THE GRADUATE SCHOOL
OF THE UNIVERSITY OF FLORIDA IN PARTIAL FULFILLMENT
OF THE REQUIREMENTS FOR THE DEGREE OF
MASTER OF SCIENCE

UNIVERSITY OF FLORIDA

2010

To X, Y, and Z

ACKNOWLEDGMENTS

I would like to acknowledge my parents, Rob and Anne, for their enduring support throughout my adventures. I would like to thank my brother, Chris, and his family, Ivy and Riley, for their love and wisdom. Amr Abd-Elrahman, my advisor, has provided valuable guidance and input throughout this research. Bon Dewitt, Scot Smith, and the Geomatics program have provided quality resources and the opportunity to be part of a challenging learning environment. I would like to acknowledge my colleagues that have provided their time, thoughts, and efforts towards this project with special thanks to Lou Nash, Keith Dixon, Mario Hernandez, John Smith, Donna Nash, and the Measutronics Corporation. I would also like to thank Bruce Francis from Applanix, Jimmy Green and Joe Revelle from Optech, and Charles Brennan from R2Sonic.

TABLE OF CONTENTS

page

LIST OF TABLES

LIST OF FIGURES

Abstract of Thesis Presented to the Graduate School
of the University of Florida in Partial Fulfillment of the
Requirements for the Degree of Master of Science

ACCURACY EVALUATION OF TERRESTRIAL LIDAR AND MULTIBEAM SONAR SYSTEMS MOUNTED ON A SURVEY VESSEL

By

Michael Esten Dix

December 2010

Chair: Amr Abd-Elrahman
Cochair: Bon Dewitt
Major: Forest Resources and Conservation

There is an emerging demand for data that can accurately describe the transitional environment between land and water. Survey equipment and techniques are meeting this demand but their resolution and repeatability capabilities are still being addressed. This research provides a performance test of terrestrial lidar and multibeam sonar systems integrated with Global Navigation Satellite System/Inertial Navigation System (GNSS/INS) positioning and orientation on a vessel platform. To measure the accuracy of the data, experiments were designed to allow the lidar and sonar systems to acquire scans of a control target that extended above and below the water surface. The scans were acquired under normal and induced conditions present in the marine survey environment such as variations in speed, range, motion, and orientation. The scan data was post-processed to create a blended GNSS/INS solution accounting for optimal sensor position and orientation dynamics throughout data collection. The scans from each data set were viewed in point cloud software and coordinates representing the center of the target were selected. These coordinates were then compared with the control coordinates for the target and errors in northing, easting, elevation, and planimetric dimensions were calculated. Standard deviation, Root Mean Squared Error

(RMSE), and Mean were also computed across all data sets for each experiment. Horizontal RMSE values of 0.06m and 0.03m were achieved for the lidar and sonar data, respectively. Vertical RMSE results of 0.04m were found for both data types. These results were comparable with previous mobile mapping research involving similar systems. Contributing error sources are also discussed regarding expected and achieved results. The methodology and results of this research provide validation of lidar and sonar data acquired from a survey vessel.

CHAPTER 1
INTRODUCTION

In many coastal and inland waterways there exists a need for three-dimensional (3D) spatial data of features above and below the water surface to support construction, engineering, monitoring, and environmental projects. Many times this involves civil structures such as bridges, seawalls, and port areas where features necessarily extend through both environments. Current methods to acquire these data involve traditional tape measurements and the deployment of divers to more advanced combinations of land and hydrographic surveying techniques. This research evaluates the accuracy of a system that can acquire data above and below the water surface using a single survey vessel. The goal of this research is to test whether terrestrial lidar and multibeam sonar systems mounted on a survey vessel can achieve horizontal and vertical error values equal to or less than 0.05m as established by Barber (et al., 2008) for error pre-analysis estimates of a mobile terrestrial lidar system mounted on a van.

Surveying and mapping has grown in scope along with technological advances in hardware and software. Governments are requiring more spatial data concerning their lands and underwater features in a format that is comprehensive, accurate, and capable of being referenced to historic and future data. The United States Army Corps Civil Works Program (2008) estimates a 2010 fiscal year budget of $1.89 billion towards their Navigation business program which includes planning, construction, operation, and maintenance of channels, locks, dams, and other inland waterways. They also budgeted $1.32 Billion in 2010 for the Flood and Coastal Storm Damage Reduction program which includes the design and construction of dams, levees, jetties and seawalls. Shorelines and coastal areas represent a unique and changing boundary of

traditional hydrographic and topographic maps. In many situations, the ability has now met the need for a “seamless integration of recent, high-resolution topographic and bathymetric data” (Gesch & Wilson, 2002).

Mobile lidar mapping from a terrestrial platform has been developing since the early 1990's (Grejner-Brzezinska, Li, Haala, & Toth, 2004). This method of data collection is effective in its ability to capture large amounts of data quickly and accurately. Conventionally, terrestrial lidar instruments are used while mounted on a fixed tripod; only in recent years has the terrestrial lidar scanner been considered on a mobile vessel platform (Talaya et al., 2004). Due to Global Navigation Satellite System/Inertial Navigation System (GNSS/INS) positioning in real time and through post-processed kinematic solutions, there is less of a requirement to scan control targets for geo-referencing data. However, as mobile mapping environments vary significantly, scanning control targets provides a check for systematic errors as well as evaluating overall system performance in a survey area.

Sonar platforms for mapping applications were born in the mobile environment and have continued to increase in resolution and coverage. Multibeam echo sounders (MBES) have the ability to ensonify an area with spatial resolution dense enough to allow for minimal interpolation when developing a surface or elevation model. Depending on equipment configuration and range from the sensor to an object, the spatial resolution of an MBES sensor can be similar to that of a terrestrial lidar sensor. Sonar systems are difficult to test for absolute accuracy due to the difficulty in establishing underwater control points. Digital elevation models can be compared over multiple data sets and specific features can be analyzed in the same manner, but these

methods fall short of measuring the accuracy of a specific point that has been established by independent control. The evolution of this methodology has come to a point where the accuracy and precision of the data should be measured to continue its development. This is cardinal for understanding its suitability in many applications.

1.1 Applications

Data collected from this type of terrestrial lidar and multibeam sonar configuration is advantageous in its ability to tie into existing reference and control data. These data are currently being combined in Geographic Information Systems (GIS) but may suffer due to the variability in data sources. Gesch and Wilson (2002) note that, "because existing topographic and bathymetric data have been collected independently for different purposes, it has been difficult to use them together at the land/water interface owing to differences in format, projection, resolution, accuracy, and datums." For example, bathymetric data of major rivers in a county may be added to a GIS of that county with polygons for property lines and setbacks. This shows, in general, how the depth and location of waterways relate to property boundaries but it is typically not robust enough to derive survey measurements and interpretations.

Monitoring applications of this set-up are numerous. Current methods of assessing, categorizing, and reviewing the stability of structures that extend above and below the water surface are tedious, subjective, and many times not feasible. These structures include docks, bridges, seawalls, dams, levies, locks, and jetties. For large projects, a combined lidar and sonar system may decrease the time it would take to inspect these structures. These data can also be used for feature extraction (Manandhar & Shibasaki, 2002) and classification (McGonigle, Brown, & Quinn, 2010). Environmental applications involving coastal erosion and habitat monitoring will benefit

from the processes that can be modeled. During marine construction, many operations can be observed. As support structures are being installed, their orientation can be confirmed by control points above and below the water. For engineering, as-built surveys can also be generated and recorded. Repeatability and integration of these types of data confirm the value for its extended use in future applications.

1.2 Error Analysis

Data acquired by remote sensing instruments from a mobile platform have many sources of error. Most instruments, sensors, and equipment used in the field of Geomatics have published accuracy and precision tolerances that are used in evaluating performance (Ernstsen et al., 2006). Many times, error analysis is based on factory calibration values as well as field or "in-situ" calibration techniques. For mobile mapping systems, the primary source of positional error is expected to be kinematic GNSS positioning (Barber, Mills, Smith-Voysey, 2008). There have been significant strides in the field of surveying that established the integration of GNSS positioning with an INS for mobile surveying applications in the air, on water, and for mobility on land (Mostafa, Hutton, & Reid, 2001). Many of these systems have been able to determine their real-time position at the centimeter level while synchronizing to the timing of scanning instrument. With mobile marine platforms the accuracy of a system is often assumed to this extent, but in many surveys the actual points measured are not verified against an absolute control system.

Barber (et al., 2008) conducted an accuracy evaluation of mobile terrestrial lidar experiments. Their research was conducted in an urban environment with sensors mounted on a van driven on a paved street. In contrast to Barber, the lidar and sonar sensors in this research were mounted on a survey vessel driven in a port environment

and thus subject to increased dynamic motion. Using a formula built upon Ellum and El-Sheimy (2002), Barber established pre-analysis expected horizontal and vertical errors of approximately 0.05m at a range of 5.0m. They were able to achieve an average vertical RMS error of 0.046m with a standard deviation between 0.02m to 0.03m. Horizontally their results indicated an accuracy of approximately 0.10m. Their pre-analysis estimates did not take into account the quality of the GNSS control for their targets or the accuracy associated with selecting coordinates of the target center from the scan. However, these components were addressed in their research as contributing sources of error and are attributed to the lower than expected horizontal accuracy from their experiments.

While research to develop error budgets for a MBES system (Hare, 1995) exists, there is little on research evaluating expected and achieved absolute horizontal and vertical error of MBES systems (Ernstsen et al., 2006). In this research we use the same positioning and orientation system to test both the lidar and sonar sensors. The lever arm calibration measurements were also determined using the same procedure and equipment for both lidar and sonar sensors. The primary difference exists in sensor ranging methods and capabilities. MBES beam-forming of an acoustic pulse through water is subject to sound velocity, objects in the water, and attenuation among other influences as compared to the relatively minimal influences a laser (from a terrestrial lidar instrument) encounters through the medium of air. The raw range resolution, or accuracy of the measured distance from sensor to an object, of the MBES used in this research is slightly (<0.01m) larger than that of the lidar. The methods of calibrating the angular orientation offsets of each sensor reference frame to the Inertial Measurement

Unit (IMU) reference frame are quite different as described in sections 3.4 and 3.5 of this paper. Recognizing these similarities and differences, the pre-analysis horizontal and precision error estimates established by Barber (et al., 2008) were considered also against the MBES results of the experiments in this research.

The pre-analysis estimates involved a geo-referencing formula (Figure 1-1) expanded from Ellum and El-Sheimy (2002) that can be visually represented (Figure 1-2) to describe possible sources of error. The position vector of the GPS antenna in the mapping frame at time *t* describes the position solution from the GPS receiver and is where the first measurement error source is found. The rotation matrix between the IMU frame and the mapping frame at time *t* will introduce error from the GPS heading solution determined between the two GPS antennas and from the dynamic motion measurements of the IMU. Errors from lever arm offsets are present in the position vector of the sensor (terrestrial lidar or MBES) in the IMU frame and from the position vector of the GPS antenna in the IMU frame. Angular errors from the rotation matrix between the sensor frame and the IMU frame are a result of the boresight procedure (for the terrestrial lidar) and the patch test (for the MBES). The determination of the object point in the sensor frame involves error from the sensor's (terrestrial lidar or MBES) ranging accuracy at a particular angle off nadir, or center.

1.3 Background

1.3.1 Terrestrial Lidar

An advantage of a terrestrial lidar instrument mounted on a vessel is that it can be operated using the same positioning and orientation system as a MBES. Some software programs offer real-time viewing of lidar data during acquisition. This can

provide instantaneous data coverage analysis. If the data collected is not enough or not correct, a quick determination can be made to do the survey again.

The lidar instrument can be mounted on a survey vessel in a fixed position, programmed to repeatedly scan a vertical swath. Thus, as the boat moves forward, the scanner is imaging in a fixed direction against the changing landscape as the vessel moves by. Stewart and Canter (2009) wrote that, “A marine vessel affords a unique perspective from which to capture these near-shore structures and topography, providing a viewpoint impossible from the land or air”. The scanner can be optimized for a particular project in its calibration and settings. The vertical swath width (angle) can be changed to cover more or less area. The sensor rotation angle between laser pulses can also be increased or decreased to control the amount of points along the swath. If the settings are too sensitive there may be too much noise in the data creating false edges or layers. Conversely, if too little data is collected, there may not be enough points to model a surface, line, corner, and other types of targets.

1.3.2 Multibeam Echosounder

There are a few types of sonar instruments that can acquire a three dimensional target. For this research a MBES was selected for accurate range resolution, effective integration with a position and orientation system, and its comprehensive swath coverage similar to a terrestrial lidar sensor. A MBES transmits an acoustic pulse that generates multiple range returns from an object or objects. These returns, or "beams" are spread out to achieve an opening angle up to 160 degrees to cover a large area or they can be focused to within a few degrees. Similar to the lidar instrument, the angular range that the beams are spread over is referred to as the "swath width". As the boat moves forward these swaths collect data points within the coverage area. While the

lidar scanner pulse rotates along a swath width at an extremely high pulse rate of 10,000Hz (Applanix, 2009), the MBES determines all the points along its swath from one pulse at a relatively lower pulse rate up to 60Hz (R2Sonic, 2010). Mounted to the vessel underwater, the MBES can be positioned in many ways to face down, sideways, or forward to collect data from a desired perspective.

1.3.3 Sensor Positioning and Orientation

The scanning devices (lidar and sonar) were securely attached to a moving vessel and thus subject to angular motion on all three axes and positionally with respect to a three-dimensional coordinate system. Without correction for vessel movements on the water, the data obtained from the scanners would be disoriented. An inertially-aided GNSS system was used to provide the positioning and orientation of the mobile platform throughout data collection. To configure the system, each sensor was mounted securely to the vessel. Three-dimensional distance offsets were measured to relate each sensor to the IMU. The positioning and orientation system establishes a precise heading vector that was integrated with yaw motion measurements during data acquisition. A calibration for the lidar (boresight) and sonar (patch test) sensors were carried out to determine the angular orientation offsets with respect to the IMU. The value of an integrated GNSS/INS system is in their complementary measurements. Mostafa, Hutton, and Reid (2001) described this by saying, “the GPS position and velocity errors are bounded and noisy, while the inertial navigator errors grow unbounded but are essentially noise free. The GPS can thus be used to estimate and correct the errors in the inertial navigation solution.”

The system can compute a real-time solution as well as a post-processed smoothed best estimate of trajectory (SBET) that can be applied to the lidar and sonar

ranging data. The post-processed kinematic (PPK) solution was used in this research to achieve the highest accuracy. Another reason that this platform was chosen was that the lidar and sonar sensors were integrated with the same positioning and motion compensation system. The acquired data also went through similar post-processing procedures. If there is a systematic error somewhere in the system it will be easier to find with shared system components. This may help in tying together the accuracies of both systems better than if they were acquired separately. While this may imply that the sonar and lidar data must be acquired simultaneously during the same pass, many times the sonar may need to make multiple passes while the lidar may only need one. Or, the lidar instrument may need to be further away from the shore to capture a desired target while the MBES may need to be as close as possible for the same purpose. While simultaneous data collection may be ideal, it is not necessary and is sometimes impractical for the best and most comprehensive data coverage and resolution.

$$r_p^m = r(t)_{\text{GPS}}^m + R(t)_{\text{IMU}}^m (r_s^{\text{IMU}} - r_{\text{GPS}}^{\text{IMU}} + d_p^s R_s^{\text{IMU}} \hat{r}(t)_p^s).$$

Where:

r_p^m	is the position vector of the object point in the mapping frame (m)
$r(t)_{\text{GPS}}^m$	is the position vector of the GPS antenna in the mapping frame at time t
$R(t)_{\text{IMU}}^m$	is the rotation matrix between the IMU frame and the mapping frame at time t
r_s^{IMU}	is the position vector of the sensor in the IMU frame
$r_{\text{GPS}}^{\text{IMU}}$	is the position vector of the GPS antenna in the IMU frame
R_s^{IMU}	is the rotation matrix between the sensor frame and the IMU frame
d_p^s	is the range observed by the sensor to the object point
$\hat{r}(t)_p^s = \begin{pmatrix} \cos(\theta) \\ 0 \\ \sin(\theta) \end{pmatrix}$	is the unit vector point in the direction of the object point in the sensor frame at time t where θ is the scan angle.

Figure 1-1. General geo-referencing formula (Barber et al., 2008) for terrestrial lidar and Multibeam Echosounder (MBES) system.

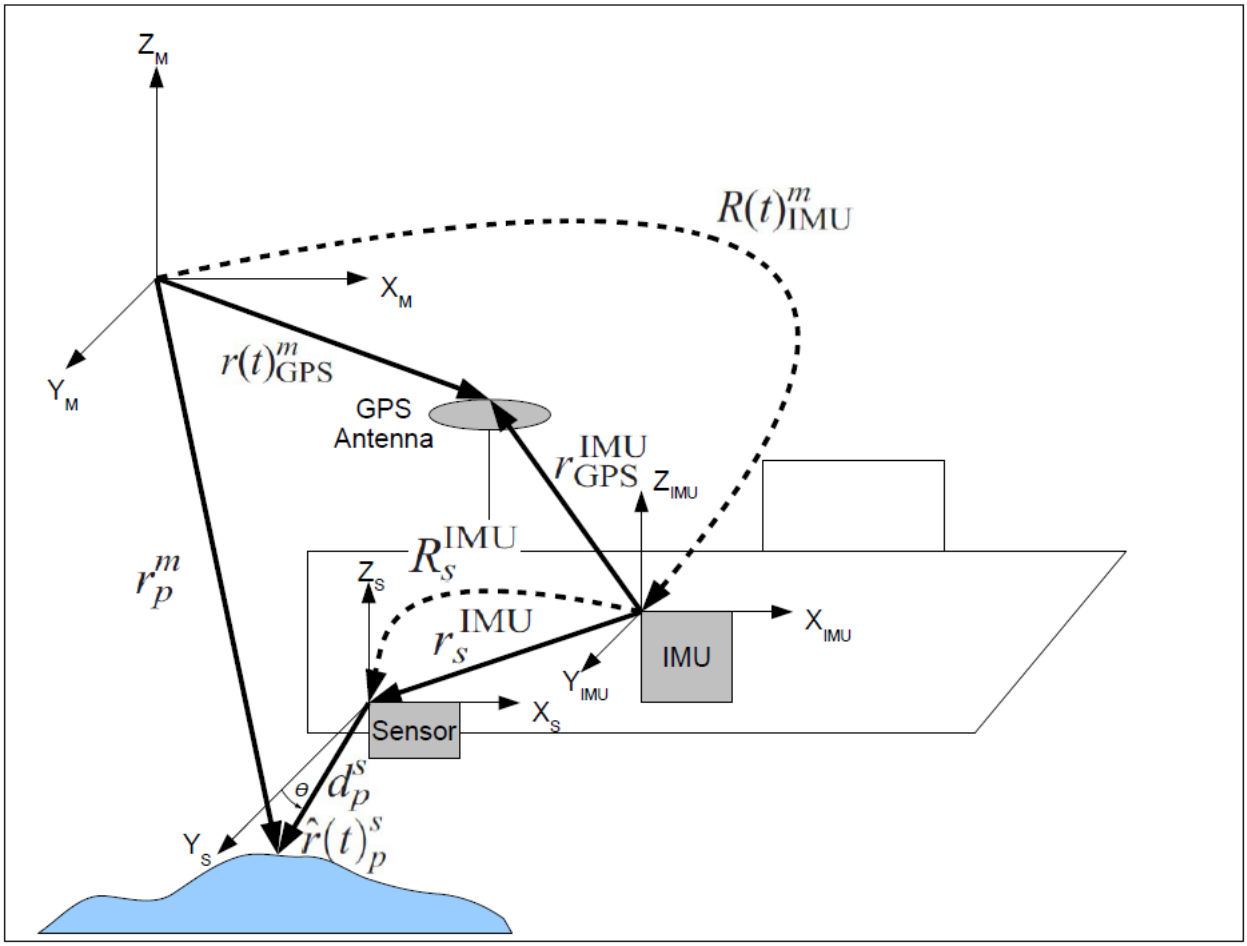

Figure 1-2. Visual representation of geo-referencing formula (from Figure 1-2).

CHAPTER 2
METHODOLODY

2.1 Site and Equipment

The test site was a port area in Tampa, FL (Figure 2-1) off the northwest facing side of Harbour Island. The site was chosen because of accessibility to a low concrete dock structure to which a target could be mounted. The target system (Figure 2-2) was modified for each of the experiments and consisted of a long rod that extended above and below the water. On the section above the water a lidar target was attached to the rod to allow for coordinate extraction of the target center during post-processing analysis. Below the water there was a sonar target to provide the same result.

GPS receivers were used to help establish control for the project. A Trimble SPS882 Smart GPS Antenna was mounted on the target. This unit has the receiver and antenna in the same housing and is designed to be mounted directly on top of a survey rod. This receiver was configured to log data internally to be post-processed against a base station or network. The target was designed in this way so that only minor offsets needed to be applied to the horizontal (X and Y) coordinates of the targets. An offset for the Z-axis was measured from the Antenna Reference Point (ARP) down to the vertical center of the lidar and sonar targets. Another GPS receiver that was used as a local base station was a Trimble 5700 receiver with a Zephyr Geodetic antenna. A group of Continually Operating Reference Stations (CORS) was another key component in creating a control network for the experiments. The CORS network is comprised of GPS base stations set up over known points that continuously collect GPS data. This data is available for free through http://www.ngs.noaa.gov/UFCORS/ (2010) which is managed by the National Geodetic

Survey (NGS) under the direction of the National Ocean Service office of the National Oceanic and Atmospheric Administration (NOAA).

The lidar scanner was a LANDMark Marine instrument from Applanix. It is manufactured by Optech Inc. as an ILRIS-3D with modifications designed for mobile mapping in a marine environment. It was mounted starboard with the scanning sensor facing outward (Figure 2-3), approximately perpendicular to the centerline of the vessel. As mentioned previously, the instrument scans in a fixed direction with a vertical swath width of 40 degrees or less.

The multibeam echosounder (MBES) was a Sonic 2024 manufactured by R2Sonic. It was also mounted starboard and positioned approximately below the lidar scanner. A Sonar Interface Module was located inside the cabin and served as a junction box for the sonar head to the other sensors. The MBES faced downward (Figure 2-3) and produced a swath width across track (athwartship) of 160 degrees. Attached to the Sonic 2024 was a Valeport miniSVS sound velocity sensor. This device provided real-time sound velocity data.

The position and motion of the vessel platform was observed using an Applanix POS MV system. For positioning, the system contained a GPS receiver utilizing two Trimble Zephyr Model 2 Rugged antennas. The primary antenna was used for position and a second antenna was used to determine a heading vector. The data from the receiver was output in a standard NMEA format that is used in real time to aid in navigation of the vessel and in processing the location and orientation of the vessel and its sensors. An inertial measurement unit (IMU), also integrated into the POS MV

system, was used to measure pitch, roll, and yaw along with velocity movements horizontally and vertically (heave).

The lidar software consisted of Optech's ILRIS 3D PC Controller interface (for sensor settings and data acquisition), Match View (for boresighting), and Parser (for exporting the data). The MBES data was collected and processed in Hypack's HYSWEEP software suite. The MBES settings were controlled through R2Sonic's Sonic Control 2000 software. The positioning and orientation data was controlled and acquired by Applanix's POSView and post-processed in POSPac MMS. Quick Terrain Modeler and Pointools View Pro were used for 3D point cloud modeling.

2.2 Calibration

2.2.1 Lever Arm Offsets

Lever arm offsets of each sensor (lidar, sonar, GPS antenna) relative to the IMU were needed to reference the lidar and sonar data to its true position and to allow for motion compensation to be appropriately applied. A 1-second Trimble SPS930 total station was used to measure the coordinates of each sensor. The final coordinates were averaged from measurements taken from two different control points. The coordinate system was then rotated to the centerline of the vessel (parallel to the X-axis of the IMU) and the origin (0,0,0) moved to the reference point on top of the IMU.

2.2.2 Lidar Boresight Procedure

A boresight procedure was needed to accurately measure the angular orientation offsets of the lidar sensor with respect to the IMU for all three axes. To begin, 10 targets were set up at different locations within the sensor's field of view. The targets were spaced at varying depths, widths, and heights to create a diverse field of view

(Figure 2-4). The locations of each target were then measured by a robotic total station from two set-ups and the resulting coordinate sets were averaged.

Next, the lidar scanner (mounted on the vessel) was situated to face the targets. The POS MV was turned on and began recording data. When the POS MV had recorded data for 5 minutes, the lidar scanner was used to acquire a 3D static scan of the targets. This part of the process allowed the lidar sensor to scan targets with known coordinates while the POS MV recorded its position and orientation. The POS MV was allowed to record data for 5 minutes after the scanning was completed. POS MV data was recorded for extended periods of time to allow for the forward and backward processing involved in determining the present position and orientation solution at a given time. The lidar instrument was also receiving real-time GPS (UTC time) information along with a 1 Pulse Per Second (1PPS) signal during the scanning process to accurately time-tag each laser pulse.

The data logged from the POS MV during that session was post-processed in POSPac MMS to output a Smoothed Best Estimate of Trajectory (SBET) file. A SBET file is a post-processed solution of the position and orientation of the IMU and GNSS sensors. The lidar scan data was then loaded into a parser program, which allows geo-referencing transformation and other parameters to be applied before outputting the data in a variety of standard file formats. Here the SBET file was applied to the lidar scan of the targets and then output as an ILRIS Exchange Format (IXF) file.

The IXF file is loaded in to Match View along with the coordinate file containing the locations of each target. The Match View program allows the center of each target in the lidar scan to be visually selected and associated or registered with its respective

control coordinates that were measured by the total station. This procedure was done for each target and these associations were used to compute a resection to determine the angular orientation of the sensor. This orientation in all three axes is compared to the orientation of the IMU provided by the SBET. The angular differences between the IMU and lidar sensor are the boresight angles. The boresight angles were applied to the lidar scan data during post-processing.

2.2.3 Multibeam Patch Test

A patch test calibration for the MBES is similar to the boresight calibration for the lidar sensor in that it determines the angular orientation of the MBES with respect to the IMU. However, the procedure is much different. The patch test is a sequence of separate procedures, each designed to isolate roll, pitch, or yaw offsets between the MBES and IMU reference frames. Latency in the timing of the MBES pulse to the positioning and orientation system can also be measured. While the procedures are separate, a calibration error in one parameter could adversely affect the results of another parameter. The data for this research was acquired using HYSWEEP software. HYWEEP has a patch test module that aides in determining these parameters by exploiting angular errors between certain data sets. Latency is for this system is assumed to be zero as the sonar data is UTC time-tagged with a 1PPS signal directly from the POS MV system.

The pitch test consisted of two MBES data sets collected over the same line in opposite directions at the same speed over a relatively sloped bottom surface. The second test was for roll offset. Two MBES data sets were collected over the same line in opposite directions at the same speed over a relatively flat surface. The final test

was for yaw offset. Two MBES data sets were collected over parallel lines at the same speed over flat area that included a sloping feature.

2.3 Variable Conditions

The experiments designed for this study placed the measurement systems under varying conditions of speed, range, motion, orientation, and repeatability while the target was scanned. Some of the data sets were collected under normal or “standard” conditions. These standard conditions were slow speed (2 knots), close range (3m), normal boat motion, scan direction perpendicular to the face of the target (Figure 2-5), and consisted of one pass by the target. All data sets were assumed to be acquired under these conditions unless a variable condition was applied.

The speed variable conditions were typical of hydrographic surveying; this research evaluated a speed range of slow (2 knots), medium (3-4 knots) and fast (5-6 knots). The ranges consisted of close (5m), medium (10m) and far (15m). Since the target was scanned from the side and at a shallow depth, the MBES was limited in range. The MBES swath width can be opened to a maximum of 160 degrees and the further away from the target it is, the lower its field of view will be towards an object extending vertically down from the water surface.

With regard to angular motion on all three axes, a vessel is subjected to pitch, roll, heading. As these motion parameters are unavoidable, they constitute necessary conditions of each experiment. While many coastal areas are subjected to extreme amounts of motion, many inland marine environments are relativity stable. The latter environment was chosen for this research to allow for the most accurate achievable results. However, a condition variable was designed to create an extreme amount of roll motion. This was a simple variable to create by rocking the vessel from side to side

as the vessel passed by the target and would offer insight in to what effects this magnitude of motion may have. Another motion condition to be evaluated was to scan the target immediately after the vessel finished making a turn. One of the experiments was also designed for the vessel to pass by the target at a 45 degree angle off perpendicular. Acquiring multiple target scans during continuous data collection of one data set was also invoked to assess variability.

2.4 Data Collection

2.4.1 Experiment 1

The target was set-up and attached to a concrete dock outcropping and leveled. It consisted of a 5m steel rod mounted to a dock. On the section above the water, a 35cm x 43cm rectangular lidar target was attached to the rod (Figure 2-6). The target was made out of hard plastic and checkered with aluminum tape to give the surface contrasting reflectivity. On the section below the water, a metal disc 40cm in diameter was attached to the rod (Figure 2-7) as a sonar target. The GPS receiver on top of the target was started and began logging a static session. Vertical offset measurements were taken using measuring tape from the antenna reference point (ARP) of the GPS receiver to the center of both the lidar and sonar targets. A base station was also set-up nearby (<1km away). For the first experiment, 12 data sets were collected. All data sets were collected under standard conditions as described in section 2.3 unless a variable condition was applied (Table 2-1).

2.4.1.1 Control coordinate computations

The first part of processing was to establish control coordinates (actual location) of the GPS receiver that was mounted on top of the target. This receiver recorded only L1 data and could not be processed with the nearest CORS station (MCD5) due to the

baseline length of approximately 13km. A local base station had been set up <0.5km away from the target receiver and a baseline between these two points was processed to determine the control coordinates of the target receiver. The next step was to apply offsets (Figure 2-8) from the ARP of the GPS antenna to the center of each target. For the lidar data, points scanned from the survey rod were used to determine the horizontal (XY) location of the target in each data set. The offset from the center of the ARP to the edge of the rod was 0.014m. The orientation of the offset was at an azimuth of 295 degrees, so a corresponding latitude (+0.006m) and departure (-0.013m) offsets were calculated to apply to the northing and easting control coordinates, respectively. The vertical center of the lidar target was used to determine the Z coordinate in the scans. A tape measurement of that distance (-0.417m), from the ARP to the center of the lidar target, was used for the vertical offset value. For the sonar target, the same horizontal offsets as the lidar target were used. Vertically, the distance measured from the ARP to the center of the sonar target was -4.690m.

2.4.1.2 Navigation data computations

The POS MV began recording before the scanning and continued afterward for approximately five minutes. This was to ensure complete coverage for the entire scanning period. Using the POSPac MMS software, POS MV output files were imported. The base station data used above to process the target control was imported and designated as a single base station. The GNSS-Inertial Processor was executed and the resulting SBET file was exported. The GNSS-Inertial Processor combines the raw IMU and GPS data along with the base station data and incorporates a “smoother” along with the inertial navigator, Kalman filter, and error-controller components (Mostafa, Hutton, & Reid, 2001).

2.4.1.3 Lidar target scan coordinates

Using the Parser software utility, the SBET and boresight files were applied to each raw data set file. They were then exported in the WGS84-UTM 17N coordinate system in ASCII format with northing, easting, elevation, and intensity fields. Each file was then imported into point cloud software (Quick Terrain Modeler). In this software, the data set was viewed as a 3D scene and the perspective zoomed in to focus on the target as defined by a group of points. Noisy data were removed and two points were selected from the image of the target. One point was selected from the survey rod to give the best XY coordinates (Figure 2-9); another point was chosen from the vertical center of the target (Figure 2-10). For the vertical point selection, the points were displayed to show intensity values making it easier to discern the center of the target from the checkered reflective tape pattern.

2.4.1.4 Multibeam Echosounder (MBES) target scan coordinates

Each MBES data set was imported into HYPACK Multibeam Editor (MBMAX). Here the appropriate lever arm offsets and patch test angular offsets were entered. The SBET was applied and the data exported as an ASCII point file with northing, easting, and elevation fields. In HYPACK, depths (elevation) are typically positive in the downward Z direction so the elevation field was inverted during the export process. Each data set was then imported and viewed in Quick Terrain Modeler software so the horizontal and vertical target coordinates could be selected.

The sonar data produced unusable results. For each data set, there were not enough points acquired to produce an image of the target for analysis. This was likely due to a few factors. The circular target had a slight concaving edge and may have caused errant returns back to the sonar receiver resulting in sections of target to be

recorded at incorrect distances. The point density captured by the scan was also lower than desired for analysis. At an average spacing of 5cm horizontally and vertically between points, it would be difficult to determine and select a point at the center.

2.4.2 Experiment 2

A second experiment was conducted at a later date to collect data for sonar only. The experiment procedures were similar to Experiment 1. Settings for the MBES were changed to reduce the swath width to 40 degrees (instead of 160 degrees) and steer it toward the target. These adjustments increased the vertical resolution of data points ensonified on the target. The pulse rate was also increased to provide increased horizontal point density. The target structure was modified to have only one target mounted underwater for the sonar. The actual target was changed from a metal disc to a metal “X” mounted to the bottom of the rod (Figure 2-11). Aluminum tape was used along with zip ties to secure the target. For the second experiment, 14 data sets were collected. All data sets were collected under standard conditions as described in section 2.3 unless a variable condition was indicated (Table 2-2).

2.4.2.1 Control coordinate and navigation data computations

The target was not set up in the same location as the first experiment so new control needed to be established. A GPS baseline was processed between the GPS receiver from the top of the target and a local base station. Offsets were then calculated by taking the distance of 0.028m from the center of the ARP to the edge of the target and applying it to an azimuth of 295 degrees to produce a departure of -0.025m and latitude of +0.012m. The vertical offset measured from the ARP of the GPS antenna to the center of the target was -4.00m. Three SBET files were created for this survey period. Data sets 1 to 10 were processed with the first SBET file; data sets 11 to

13 were processed with the second SBET file; data set 14 was processed with the third SBET file. The POS MV system was restarted between the three successive data sets to create more independence between the data.

2.4.2.2 MBES target scan coordinates

Each SBET file was applied to the corresponding data sets in HYSWEEP along with the lever arm offsets. The data was exported and viewed in point cloud software to select coordinates for the center of the target. While the arms of the “X” target did not return complete results, the center of the target that was wrapped in aluminum tape returned consistent results. As this was ultimately the desired section of the target, this was used to select the center point of the target in each data set (Figure 2-12).

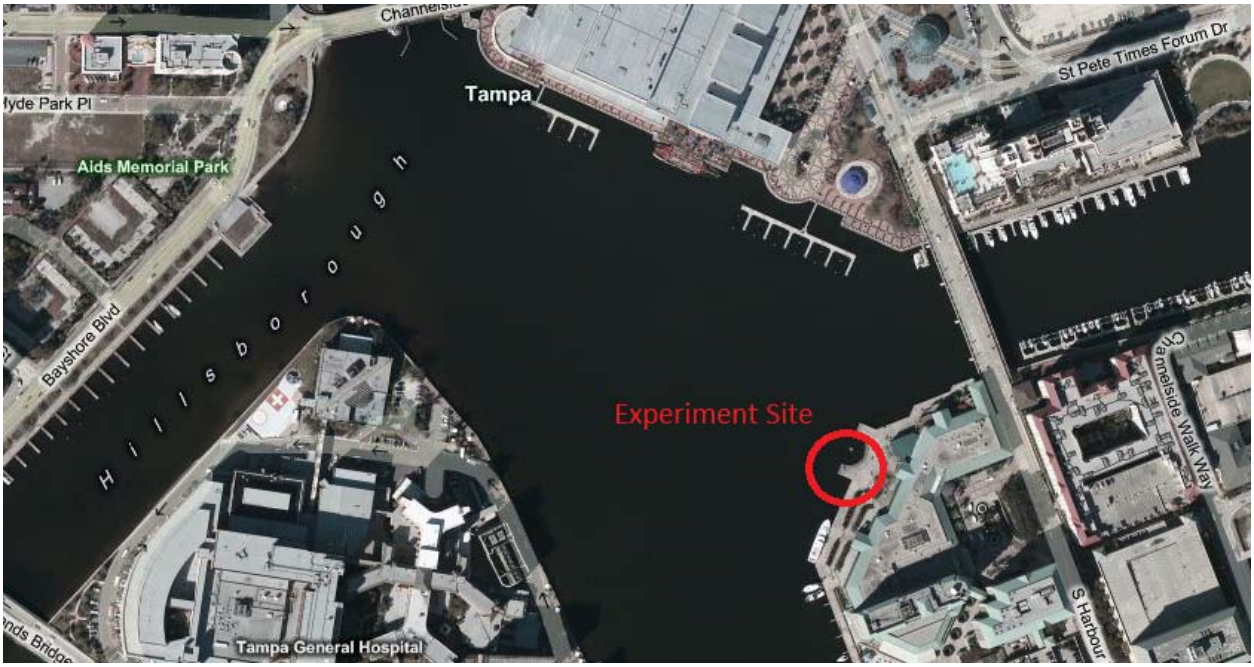

Figure 2-1. Experiment site location map. (Note: Image retrieved from Microsoft Bing Maps, 2010).

A

B

Figure 2-2. Target system A) on its side to measure offsets before installation and B) installed on a concrete dock.

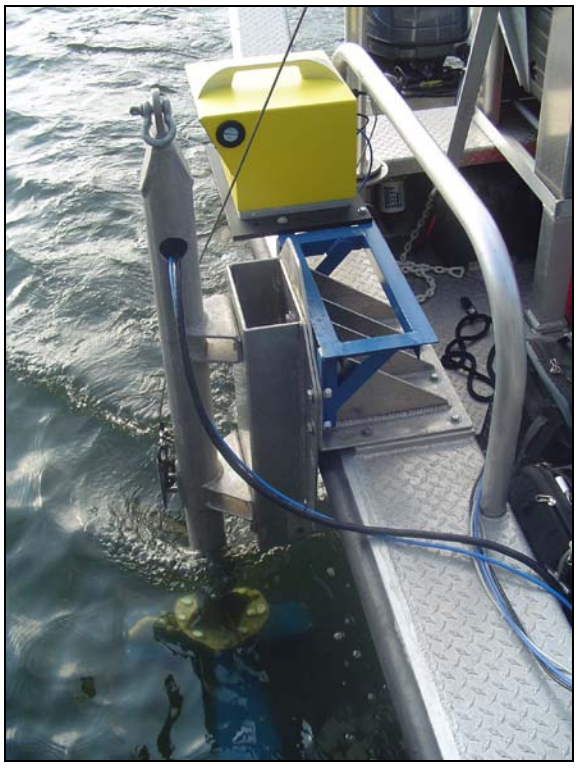

Figure 2-3. Terrestrial lidar and MBES sonar instruments mounted on survey vessel

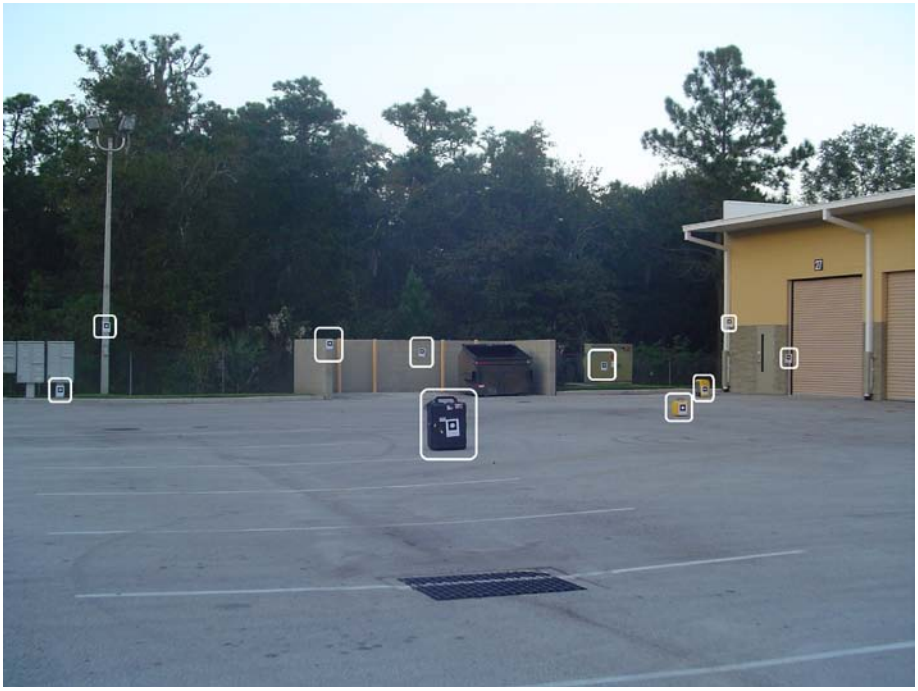

Figure 2-4. Target locations for boresight procedure.

Figure 2-5. Experiment site showing vessel course and scan direction with respect to the face of the target. Angular orientations and linear features shown here are approximate and not to scale. (Note: Background image retrieved from Microsoft Bing Maps, 2010).

Figure 2-6. Lidar target for Experiment 1

Figure 2-7. Sonar target for Experiment 1

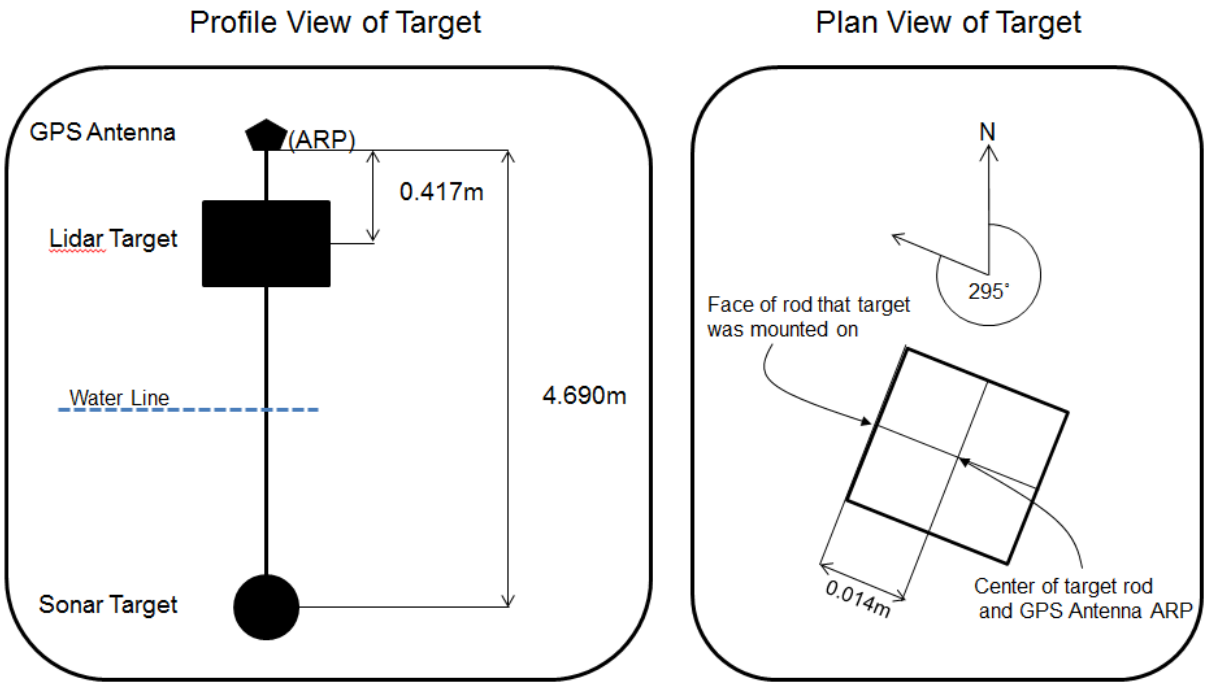

Figure 2-8. Profile and plan views of the target system with vertical and horizontal offsets, respectively. Note: Angular orientations and linear features shown here are approximate and not to scale.

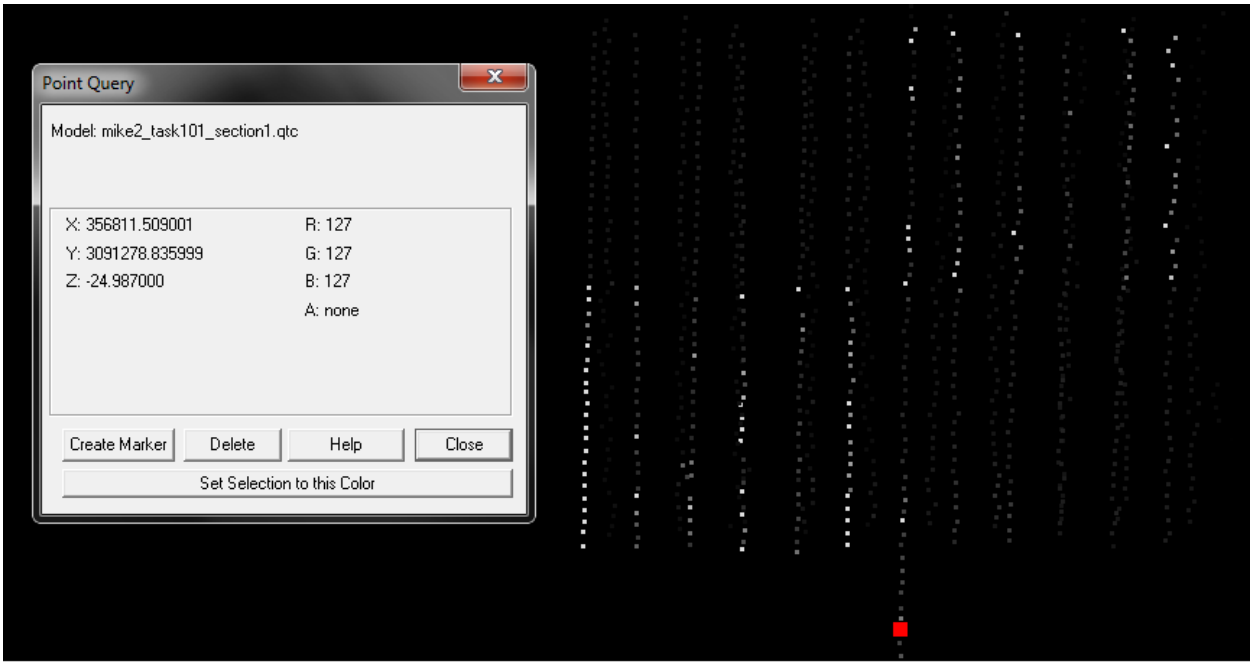

Figure 2-9. Example of XY (horizontal) coordinate selection of lidar target, Experiment 1

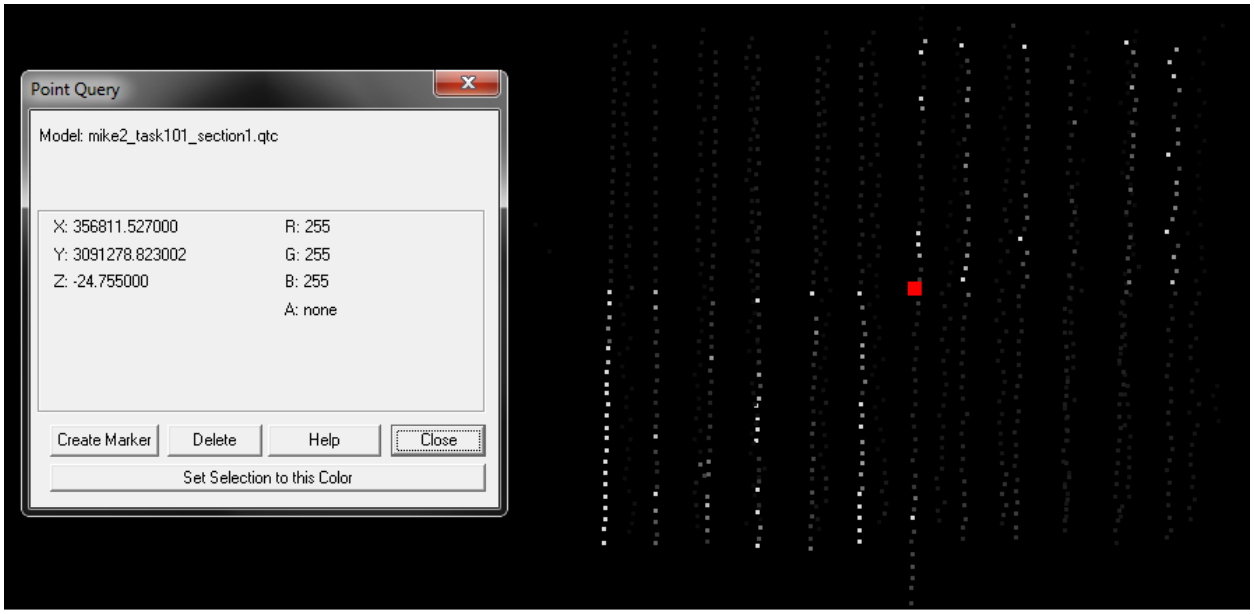

Figure 2-10. Example of Z (vertical) coordinate selection of lidar target, Experiment 1

Figure 2-11. Sonar target for Experiment 2

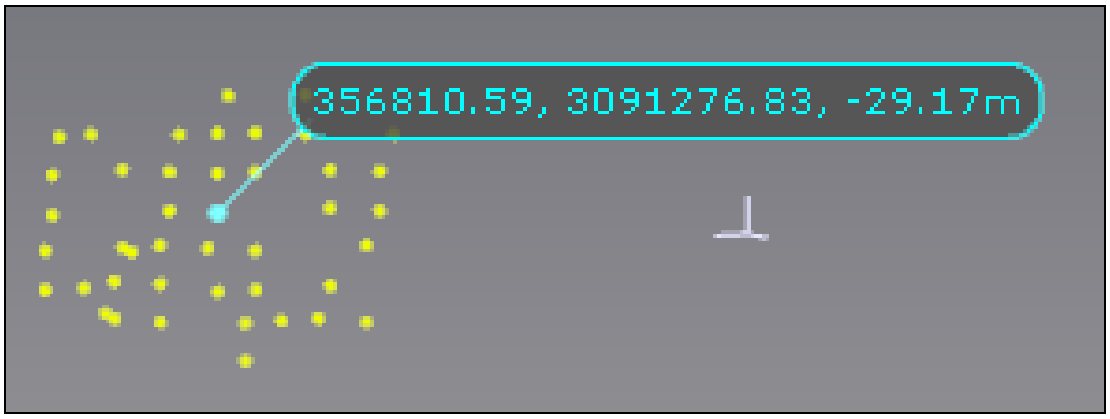

Figure 2-12. Example of XYZ coordinate selection for sonar target, Experiment 2.

Table 2-1. Variable conditions for Experiment 1

Data Set	Variable Condition	Abbreviation
1	Standard	(STANDARD)
2	Three passes of target during continuous data recording	(MULT PASSx3)
3	Medium speed	(MED SPD)
4	Maximum speed	(MAX SPD)
5	Medium range	(MED RANGE)
6	Far range	(FAR RANGE)
7	Scanned after making a slow turn, medium speed	(SL TRN MED)
8	Scanned after making a hard turn, maximum speed	(HD TRN MAX)
9	Scanned after making a hard turn, maximum speed	(HD TRN MAX)
10	Heavy side-to-side rolling motion	(SIDE ROLL)
11	45 degree angle off perpendicular	(45 DEG OFF)
12	Standard	(STANDARD)

Table 2-2. Variable conditions for Experiment 2

Data Set	Variable Condition	Abbreviation
1	Standard	(STANDARD)
2	Standard	(STANDARD)
3	Standard	(STANDARD)
4	Back and Forth	(BACK FRTH)
5	Two passes of target during continuous data recording	(MULT PASSx2)
6	Three passes of target during continuous data recording	(MULT PASSx3)
7	Medium Range	(MED RANGE)
8	Heavy side-to-side rolling motion	(SIDE ROLL)
9	Heavy side-to-side rolling motion for three passes	(SIDE ROLLx3)
10	45 degree angle off perpendicular	(45 DEG OFF)
11	Standard after POS MV restart	(STANDARD)
12	Three passes of target during continuous data recording	(MULT PASSx3)
13	Standard with modified swath to 20 degrees	(STANDARD)
14	Standard after POS MV restart	(STANDARD)

CHAPTER 3
RESULTS AND ANALYSIS

Coordinates of the target center were selected for each of the data sets. The error between those coordinates and the control coordinates for northing, easting, ellipsoid height, and horizontal distance are expressed as North, East, Vert, and Plan, respectively (Tables 3-1 and 3-2). The Plan errors represent horizontal accuracy while Vert errors represent vertical accuracy. Statistical mean, standard deviation (1σ), and RMSE were also calculated. While the data sets for each experiment were acquired under similar variable conditions, collectively they were not the same. An example of this is that the lidar data sets included two sets acquired under standard conditions and four data sets acquired under a motion variable condition. The sonar data sets included four sets acquired under standard conditions and only two under motion variable conditions. The mean, standard deviation, and RMSE represent valuable metrics to measure the overall quality of the lidar and sonar data acquired by this system, but are difficult to use in a same/same comparison with each other.

3.1 Experiment 1: Terrestrial Lidar

The average horizontal RMSE for all data sets in Experiment 1 was 0.06m with a standard deviation of 0.02m. This was 0.01cm larger than the predicted error established by Barber (et al., 2008). The average vertical RMSE was 0.04m with a standard deviation of 0.01m. The sets acquired under standard or “normal” conditions were 1 and 12. These were expected to be the most accurate as they were not subjected to any extra conditions of speed, range, motion, etc. The horizontal and vertical errors for both of these data sets were equal to or lower than the expected errors. Data set 2 shows a horizontal error of 0.05m and a vertical error of -0.05m. For

this set, the target was scanned three times during continuous data collection and is effectively the combination of three scans under standard conditions. Therefore it is not surprising that the error values for this data set were consistent with the mean errors. Both of the medium and far range data sets (5 and 6) show below average horizontal and vertical errors. If large errors existed in the boresight calibration, these errors would be magnified with increased distance from the target. No bias is shown at these ranges suggesting adequate boresight calibration.

Data sets 7, 8 and 9 were recorded after coming off a turn and had error values approximately consistent with the expected error except for the Easting error in data set 8. This error was 0.10m which was more than double the Easting errors in data sets 7 and 9. There is insufficient data available to determine if this error is random or a result of the motion variable. Data set 10 involved heavy side-to-side rolling of the vessel and sensors and created a difficult environment for the GPS and motion sensors. The GPS antennas were subjected to side-to-side movements at high velocities. The IMU would be subject to extreme motion along the roll axis which would subject the lidar sensor to rapid vertical motion. The horizontal error for this data set was 0.05m while the vertical error was -0.02m revealing no apparent degradation of accuracy from this variable condition in this instance.

The Easting error values for all data sets in Experiment 1 are positive suggesting a systematic error. This is confirmed by a t test at a significance level of 0.05 ($t_{\alpha/2}$, 0.025, 11) rejecting the null hypothesis that the mean Easting coordinate is equal to the Easting control coordinate. This phenomenon was also found in the negative vertical error values from Experiment 1. As described by the geo-referencing formula in section

1.2, possible error sources could be attributed to the terrestrial lidar sensor's dynamic ranging accuracy, GPS position and heading errors, and the errors introduced in establishing control for the target.

3.2 Experiment 2: MBES Sonar

For Experiment 2 the horizontal and vertical RMSE of 0.02m and 0.03m, respectively, are lower than the predicted error established by Barber (et al., 2008). The horizontal and vertical standard deviations for Experiment 2 are between 0.01m and 0.02m and were similar to the variability from the lidar data sets in Experiment 1. Sets 1, 4, 10, and 13 produced little or no returns on the target and could not be evaluated for this experiment. The data sets acquired under standard conditions were sets 2, 3, 11, and 14. The POS MV system was restarted just before set 11 and again before set 14. The horizontal and vertical error ranges for these data sets extend out to two standard deviations (95%) from the mean error. This suggests that the majority of the variability between all data sets was not due to the variable conditions. Sets 5 and 6 were acquired by scanning the target two and three times, respectively, during continuous data collection. The absolute horizontal errors were between 0.01m and 0.02m. Set 5 had a higher than average vertical error of 0.05m. A higher than average vertical error of 0.06m was also seen in data set 12 , which consisted of three scans of the target. The lidar sets in Experiment 1 acquired under multiple passes did not show this degradation in vertical precision.

Data sets 8 and 9 were acquired while the vessel was subjected to heavy side-to-side rolling. Set 8 had the highest vertical error (0.07m) in all the data sets in Experiment 2 while set 9 produced an error equal to the mean error for all sets in Experiment 2. All of the vertical errors, except for one (set 11), were positive and

suggests a systematic error. This is confirmed by a t test at a significance level of 0.05 ($t_{\alpha/2}$, 0.025, 9) rejecting the null hypothesis that the mean Vertical coordinate value is equal to the Vertical control coordinate. The Easting errors in Experiment 2 suggest a similar systematic error.

3.3 Lidar vs. Sonar

The average errors in the lidar and sonar data sets (Figure 3-1) reveal positive systematic errors in Easting values. As the average errors are both positive, there may be a common source that was contributing to these results. This researcher believes that during the system calibration procedures, orientation errors between the lever arm offset measurements, IMU, and GNSS receiver reference frames could have been introduced. At a 5 meter range to target, a 0.25 degree error in this rotation would introduce a 0.02m systematic error in horizontal position. The standard deviations for the lidar and sonar data sets (Figure 3-2) cannot be proven to be significantly different using an F test at a significance level of 0.05 ($F_{\alpha/2}$, 0.025, 11, 9).

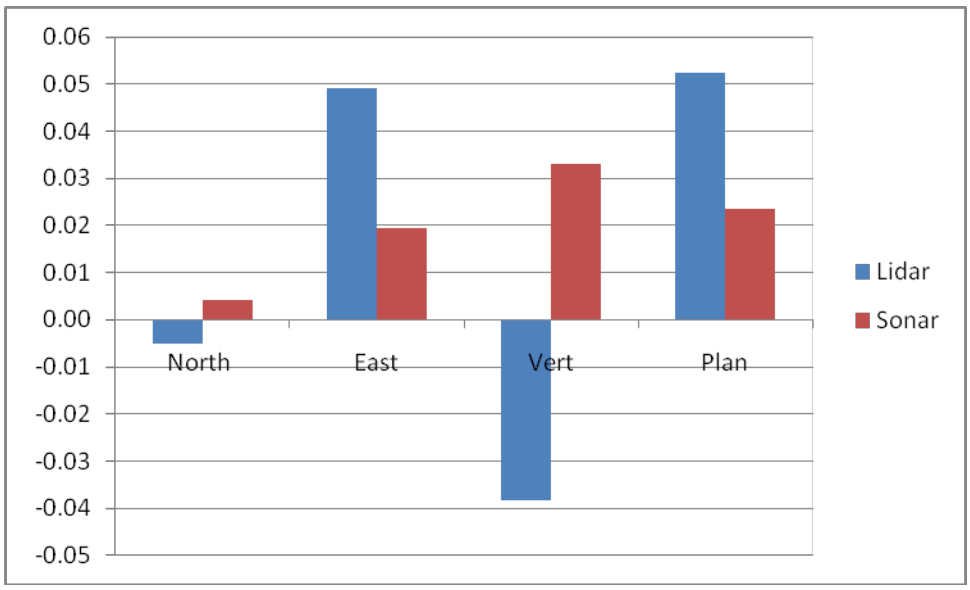

Figure 3-1. Mean error (in meters) in lidar and sonar data sets.

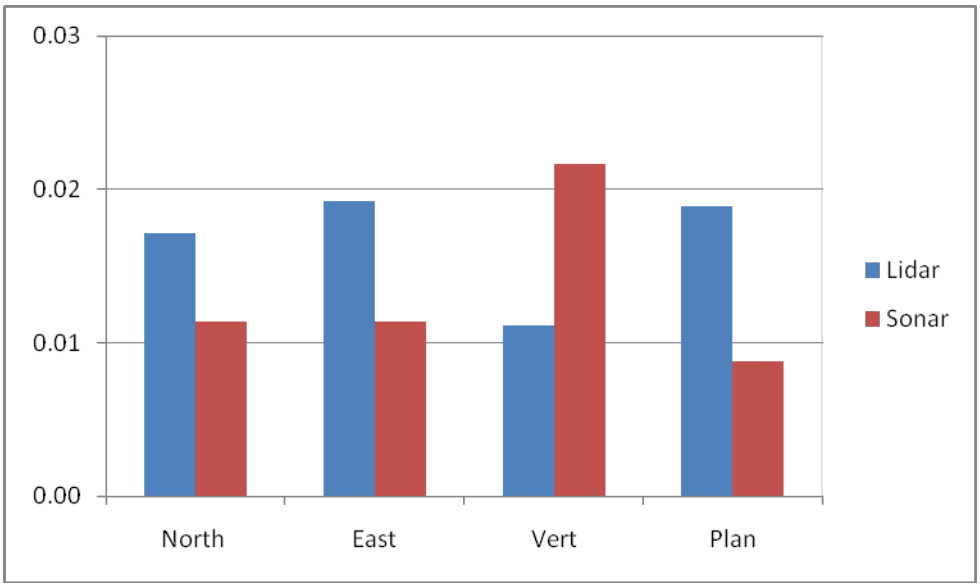

Figure 3-2. Standard deviation (in meters) in lidar and sonar data sets.

Table 3-1. Terrestrial lidar accuracy, Experiment 1 (in meters).

Data Set	Conditions	North	East	Vert	Plan
1	STANDARD	-0.03	0.04	-0.04	0.05
2	MULT PASSx3	-0.02	0.04	-0.05	0.05
3	MED SPEED	0.00	0.04	-0.03	0.04
4	MAX SPEED	-0.03	0.03	-0.03	0.04
5	MED RANGE	0.00	0.04	-0.03	0.04
6	FAR RANGE	0.00	0.04	-0.04	0.04
7	SL TRN MED	0.01	0.04	-0.03	0.05
8	HD TRN MAX	-0.01	0.10	-0.04	0.10
9	HD TRN MAX	-0.01	0.04	-0.04	0.04
10	SIDE ROLL	-0.02	0.04	-0.02	0.05
11	45 DEG OFF	0.03	0.05	-0.06	0.06
12	STANDARD	-0.01	0.02	-0.05	0.02
Mean		-0.01	0.05	-0.04	0.05
Standard Deviation		0.02	0.02	0.01	0.02
Root Mean Squared Error		0.02	0.05	0.04	0.06

Table 3-2. Multibeam Echosounder (MBES) sonar accuracy, Experiment 2 (in meters)

Data Set	Conditions	North	East	Vert	Plan
1	STANDARD	—	—	—	—
2	STANDARD	-0.01	0.02	0.03	0.03
3	STANDARD	0.02	0.00	0.05	0.02
4	BACK FRTH	—	—	—	—
5	MULT PASSx2	-0.01	0.01	0.01	0.02
6	MULT PASSx3	0.01	0.01	0.05	0.01
7	MED RANGE	0.00	0.02	0.03	0.02
8	SIDE ROLL	0.01	0.02	0.07	0.02
9	SIDE ROLLx3	0.01	0.02	0.03	0.04
10	45 DEG OFF	—	—	—	—
11	STANDARD	0.02	0.01	0.00	0.02
12	MULT PASSx3	0.01	0.02	0.06	0.02
13	STANDARD	—	—	—	—
14	STANDARD	0.02	0.03	0.04	0.04
Mean		0.00	0.02	0.03	0.02
Standard Deviation		0.01	0.01	0.02	0.01
Root Mean Squared Error		0.01	0.02	0.04	0.03

CHAPTER 4
CONCLUSION

Under varying conditions of speed, range, motion, orientation, and repeatability the lidar data from Experiment 1 and the sonar data from Experiment 2 achieved horizontal and vertical average errors equal to or lower than the error pre-analysis estimates of 0.05m by Barber (et al., 2008). The RMSE values are also within the pre-analysis estimates with the exception of the horizontal RMSE (0.06m) for lidar data in Experiment 1. For both experiments, the SBET solution for position and orientation has average horizontal and vertical RMSE values of approximately 0.01cm. The remaining average error, 0.01cm – 0.05cm, is attributed to calibration procedures (lever arm, boresight, and patch test), dynamic sensor ranging, and the quality of the target control coordinates. It is recognized that more data sets will help to establish trends caused by the condition variables and may indicate the cause of systematic calibration errors. Future research that can capture and analyze scans of the same target center by both lidar and sonar will also be helpful in strengthening accuracy evaluation for these systems.

LIST OF REFERENCES

Applanix Corporation. (2010). *LANDMARK Marine specifications*. Ontario, Canada.

Barber, D., Mills, J. & Smith-Voysey, S. (2008). Geometric validation of a ground-based mobile laser scanning system. *ISPRS Journal of Photogrammetry and Remote Sensing, 63*, 128–141.

Canter, P., Brennan, R., & Van Den Ameele, E. (2008). Proceedings of the Canadian Hydrographic Conference and National Surveyors Conference: *Tightly integrated inertially-aided post processed virtual reference station technique for marine hydrography*. Victoria, BC, Canada.

Department of the Army Corps of Engineers Civil Works Program. (2008). *Five-year development plan: Fiscal year 2009 to fiscal year 2013* (pp. 19–24). Washington, D.C.

Department of the Army Corps of Engineers. (2002). *Engineering and design – Hydrographic surveying*. (EM 1110-2-1003). Washington, D.C.

Ellum, C., El-Sheimy, N., (2002). Land-based mobile mapping systems. *Photogrammetric Engineering and Remote Sensing*, 68 (1), 13–17, 28.

Ernstsen, V.B., Noormets, R., Hebbeln, D., Bartholomä, Flemming, B.W., (2006). Precision of high resolution multibeam echo sounding coupled with high-accuracy positioning in a shallow water coastal environment. *Geo-Mar Lett 26* (3), 141-149.

Hare, R., (1995). Depth and error budgets for multibeam echosounding. *International Hydrographic Review, 72* (1). Monaco.

Gesch, D., & Wilson, R., (2002). Development of a seamless multisource topographic/ bathymetric elevation model of Tampa Bay. *Marine Technology Society Journal, 35* (4), 58–64.

Grejner-Brzezinska, D.A., Li, R., Haala, N., & Toth, C. (2004). From mobile mapping to telegeoinformatics: Paradigm shift in geospatial data acquisition, processing, and management. *Photogrammetric Engineering & Remote Sensing, 70* (2), 197–210.

Manandhar, D., & Shibasaki, R., (2002). Proceedings of Symposium on Geospatial Theory: *Auto-extraction of urban features from vehicle-borne laser data*. Ottawa, Canada.

McGonigle, C., Brown, C. J., & Quinn, R. (2010). Insonification orientation and its relevance for image-based classification of multibeam backscatter. *ICES Journal of Marine Science, 67*. (1010–1023).

Microsoft Bing Maps. (2010). [Digital aerial photograph of Tampa, FL]. Retrieved from http://www.bing.com/maps/

Mostafa, M., Hutton, J., & Reid, B., (2001). Proceedings of Photogrammetric Week '01: *GPS/IMU products – the Applanix approach*. Heidelberg, Germany: Wichmann Verlag.

National Oceanic and Atmospheric Administration. (2010). *User friendly CORS* [Data file]. Retrieved from http://www.ngs.noaa.gov/UFCORS/

R2Sonic, LLC. (2010). *Sonic 2024/2022 broadband multibeam echosounders operation manual, V2.0*. Santa Barbara, CA.

Stewart, P., & Canter, P., (2009). Feature: Creating a seamless model. *Professional Surveyor Magazine*, 29 (8). Retrieved from http://www.profsurv.com/magazine/article.aspx?i=70304

Talaya, J., Alamus, R., Bosch, E., Serra, A., Kornus, W., & Baron, A. (2004). Proceedings of XXth ISPRS Congress, Commission 5: *Integration of a Terrestrial Laser Scanner with GPS/IMU Orientation Sensors*. Istanbul, Turkey.

BIOGRAPHICAL SKETCH

Michael Dix graduated from the University of Florida in 2004 with a bachelor's degree in business administration. He has worked in the residential construction and land surveying industries and most recently has been involved with systems integration for marine construction and hydrographic surveying. He began his graduate studies at the University of Florida in 2009.